



ELSEVIER

International Journal of Mass Spectrometry 185/186/187 (1999) 221–226



# Orthogonal electron impact source for a time-of-flight mass spectrometer with high mass resolving power

Y.H. Chen<sup>a</sup>, M. Gonin<sup>b</sup>, K. Fuhrer<sup>b</sup>, A. Dodonov<sup>c</sup>, C.S. Su<sup>a</sup>, H. Wollnik<sup>b,\*</sup>

<sup>a</sup>Department of Nuclear Science, National Tsing-Hua University, Taiwan, ROC

<sup>b</sup>II. Physikalisches Institut der Universität Giessen, Heinrich-Buff-Ring 16, 35392 Giessen, Germany

<sup>c</sup>Institut für Chemical Physics, Russ. Acad. Science, Chernogolovka, Russia

Received 26 May 1998; accepted 15 August 1998

## Abstract

A compact orthogonal ion source has been developed for the gas analysis in time-of-flight mass spectrometers with the goal to use such a system for the investigation of cometary gases. An extraordinary mass resolving power of  $m/\Delta m \geq 10\,000$  and low detection limits have been obtained in a 1.3 m long instrument. (Int J Mass Spectrom 185/186/187 (1999) 221–226) © 1999 Elsevier Science B.V.

**Keywords:** Time-of-flight mass spectrometer; Ion source; Electron impact

## 1. Introduction

With the aid of modern electronic techniques, time-of-flight mass spectrometers (TOF MS) have become powerful mass analyzing tools because of their capability of rapid delivery of full mass spectra with a theoretically unlimited mass range. However, the fact that with electron impact ion sources only limited mass resolving powers  $m/\Delta m$  and modest signal-to-noise ratios were obtained from time-of-flight mass analyzer, has limited the applications [1].

The mass resolving power

$$\frac{m}{\Delta m} = \frac{t}{2\Delta t} \quad (1)$$

\* Corresponding author.

Dedicated to Professor Michael T. Bowers on the occasion of his 60th birthday.

is limited by a large number of contributions to the total flight time error

$$\Delta t \approx \sqrt{\Delta t_p^2 + \Delta t_l^2 + \Delta t_g^2 + \Delta t_e^2 + \Delta t_d^2 + \dots + \Delta t_v^2} \quad (2)$$

Here  $\Delta t_p$  is due to an imperfect “McLaren space focus” [2], which occurs downstream from the ion acceleration region,  $\Delta t_l$  and  $\Delta t_g$  are time errors in electrostatic lenses and grids,  $\Delta t_e$  is due to unstable power supplies,  $\Delta t_d$  is the signal width of the detection system and  $\Delta t_v$  is due to the initial thermal ion velocity or the “turn around time” [1]. This turn around time is often the most important time error

$$\Delta t_v = \frac{2mv_0}{qE} \quad (3)$$

with  $m$ ,  $v_0$ , and  $q$  being mass, initial velocity in the direction of extraction and charge of the ion in

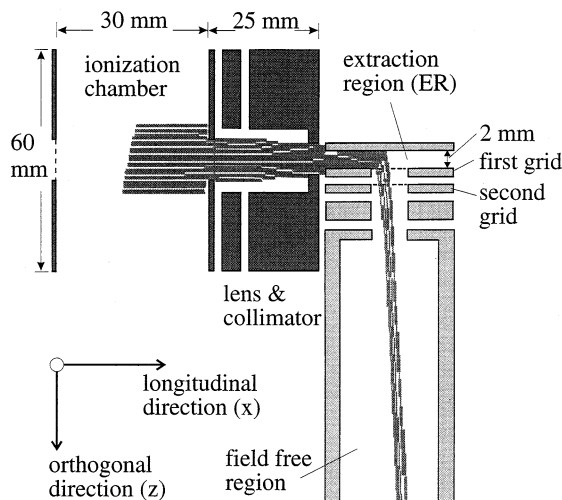


Fig. 1. Schematic arrangement of our orthogonal ion source. The transversal direction ( $y$ ) is orthogonal to the longitudinal and the orthogonal direction.

question and  $E$  being the electrostatic field strength in the ionization chamber.

To increase mass resolving power of a time-of-flight mass analyzer the flight time  $t$  must be increased or the total flight error  $\Delta t$  must be decreased [Eq. (1)]. The flight time  $t$  is increased efficiently (while keeping  $\Delta t$  constant) with an ion mirror or “reflectron” [3]. The reflectron images each mass from the McLaren focus of the ion source to the ion detector in an energy isochronous manner [4]. (In fact,  $\Delta t$  can even be reduced by compensating higher order errors of the McLaren space focus). The total time error  $\Delta t$  is reduced by reducing its main component  $\Delta t_v$ . This can be done with a higher extraction field strength  $E$  or by reducing the initial velocity  $v_0$  [Eq. (3)]. Latter is done efficiently with an orthogonally extracting ion source [5].

With the orthogonal ion source the initial velocity in orthogonal direction is reduced by extracting the ions from a low energetic primary beam ( $\approx 10$  eV) of low divergence in the direction of the extraction (Fig. 1). This type of ion source was first proposed by O’Halloran [6]. However, really effective time-of-flight mass spectrometers were built with such ion sources only later [5,7–12]. In this article we present an orthogonal ion source originally designed for analysis of cometary gases and ions. Existing ions

from the cometary atmosphere have almost thermal velocities ( $0.8$  mm/ $\mu$ s). They enter the ionization region through a grid (on left in Fig. 1) and are accelerated to form a primary beam. The filaments for the electron impact ionization are only turned on for the measurement of the cometary gases. This type of ion source can be used for any kind of gas analysis and our intention is to adapt it for GC/MS: if this source is operated with a reflectron time-of-flight mass spectrometer (see Fig. 2) we achieve very high mass resolving powers and at the same time low detection limits.

## 2. Instrument layout and principles

The new orthogonal ion source for the analysis of gases is shown in Fig. 1. It consists of: (1) the “primary beam optics” for the formation and focusing of the primary low energy beam ( $10$ – $40$  eV), which moves in the longitudinal direction and (2) the optics that accelerates these ions orthogonally to  $\approx 6000$  eV.

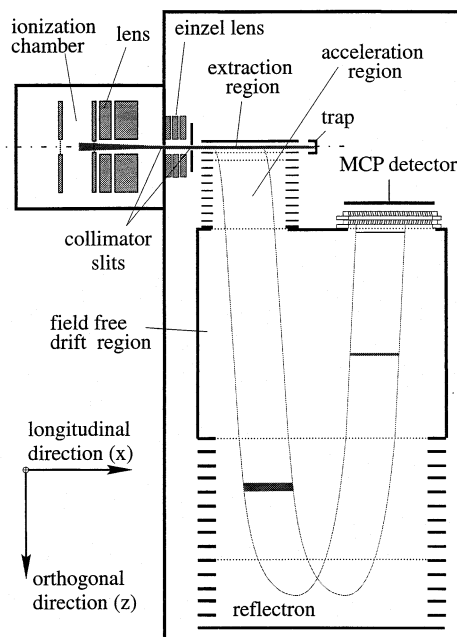


Fig. 2. Schematic diagram of a reflectron time-of-flight mass analyzer equipped with an electron impact ion source, transmission optics and an orthogonal extraction region. The primary beam optics is identical to that of Fig. 1.

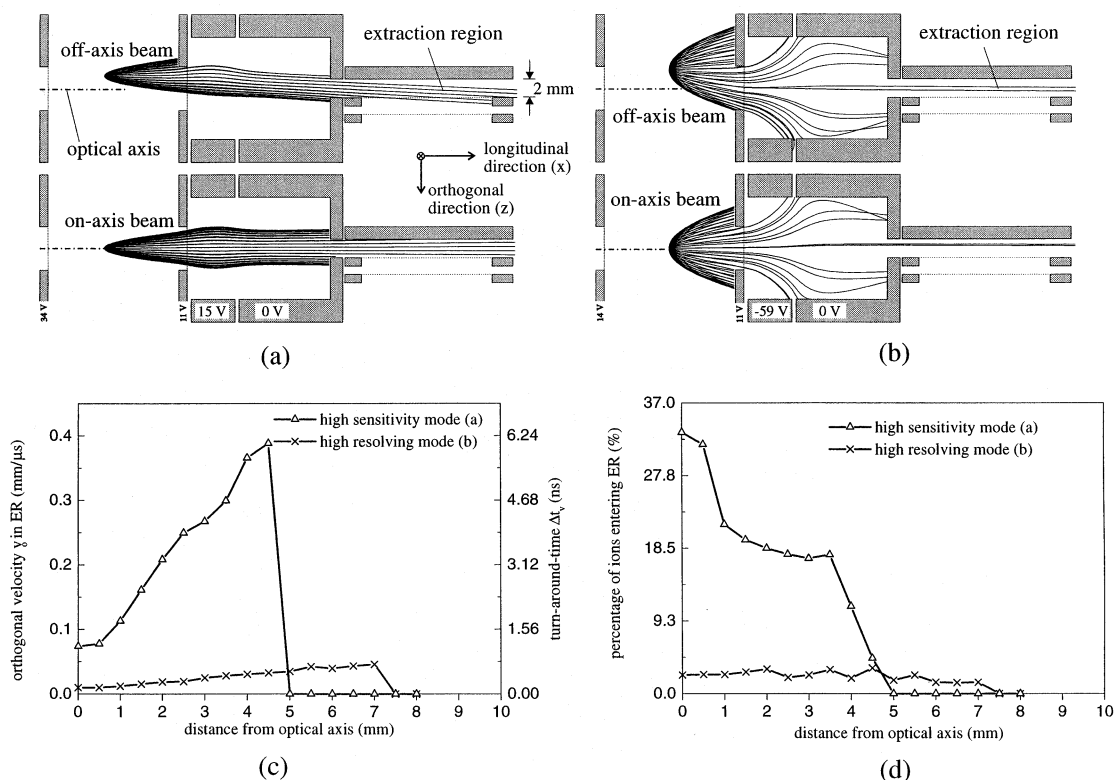


Fig. 3. Characteristics of the primary beam optics of the compact orthogonal ion source simulated with SIMION [13]. (a) In the high sensitivity mode in which more ions reach the extraction region (ER). Note here that some of the off-axis ions with larger orthogonal velocities can also sneak into the ER and limit the mass resolving power. (b) In the high resolving mode in which a more parallel beam allows higher mass resolving powers at the expense of ion intensity. (c) The orthogonal velocities  $v_0$  of ions in the ER and the corresponding turn around time  $\Delta t_v$  in dependence of the ion start position in the orthogonal direction.  $\Delta t_v$  is estimated from Eq. (3) with  $m = 127$  u and  $E = 170$  V/mm. (d) The ion intensity in the ER in dependence of the ion start position in the orthogonal direction for the two modes of operation. 40 000 singly charged ions of mass 127 u were used with isotropic initial velocity distributions corresponding to energies  $K \leq 0.04$  eV.

### 2.1. Longitudinal beam formation

This ion source was designed for the investigation of cometary gases, especially for the analysis of chemically reactive species, for which rather large dimensions are required to reduce interaction with surfaces. Therefore the ions are produced and accelerated in an open and relatively large ionization chamber and then transported to the extraction region through a collimator (see Fig. 1). In combination with the transport optics, the collimator (Fig. 1) ensures that in the extraction region the ions have only small orthogonal velocities  $v_0$  since large orthogonal velocities would increase  $\Delta t_v$ , and thus limit the achievable

mass resolving power. The primary beam optics determines the fraction of the ions that is transported into the extraction region. It can be adjusted to either a high resolving or a high sensitivity mode.

In Fig. 3 a series of ion trajectories simulated by SIMION [13] illustrates how the source operates in these two modes (see also Table 1). Both cases were calculated for singly charged ions of mass 127 with isotropically distributed velocities corresponding to initial ion energies of 0.04 eV (the particle energy at room temperature). These ions are spread longitudinally in the region of the ionizing electron beam, and are successively set off from the optic axis by steps of 0.5 mm. Fig. 3(d) displays the number of ions that

Table 1  
Numerical results from trajectory calculations for mass 127

	High sensitivity	High resolving power
$ v_0 $	0.85 mm/ $\mu$ s	0.11 mm/ $\mu$ s
$mv_0^2/2$	0.025 eV	0.0004 eV
$\Delta t_v$	5.1 ns	0.64 ns
Efficiency	10%	2%

reach the extraction region for each calculation step and Fig. 3(c) displays their orthogonal velocity distribution. Fig. 3(a) shows the ion trajectories in the high sensitivity mode and Fig. 3(b) in the high resolving mode. Note that only the off-axis groups that have the largest orthogonal velocities in the extraction region are representatively plotted in Fig. 3(a) and (b). Note also that in both modes the average orthogonal velocity in the extraction region increases with the distance of the start point from the optic axis. The high resolving mode is calculated to be characterized by 8 times lower peak velocities  $v_0$  and a 5 times lower number of ions entering the ER.

## 2.2. Orthogonal beam formation

During the “accumulation period,” when the ions in the primary beam move at low speeds into the extraction region, this region has to be field free. Even small electric fields can introduce orthogonal velocities which will limit the resolution [Eq. (3)]. Therefore the extraction region is separated from the acceleration region with two grids which prevent the field in the acceleration region (Figs. 1 and 2) from penetrating into the extraction region. During the “extraction period” two voltages of opposite polarities are applied to the backplate and the second grid of the extraction region for a short time (5  $\mu$ s).

## 2.3. Ion source operation with a mass preparation

Instead of producing a continuous primary ion beam, this beam can be modulated. It is our plan to use the primary beam as a first time-of-flight mass analyzer. With a appropriate modulation it can be avoided that low mass ions enter the drift region. When the primary beam is pulsed and the extraction

timing is late enough to let the low mass ions cross the extraction region towards the trap (Fig. 2), they will not be extracted into the drift region. When using this source in a GC/MS this would avoid saturation of the detector by the helium or hydrogen carrier gas.

## 2.4. Energy and angular ion spreads

The longitudinal velocity spread, which corresponds to an energy spread of about  $12 \pm 6$  eV will cause an angular divergence of  $\alpha_z \approx dx/dz \approx 23$  mrad after the orthogonal acceleration to 6000 eV. In the transversal direction this angular spread  $\beta_z \approx dy/dz$  is even larger. Both these divergences cause some loss in the overall transmittance.

## 3. Experimental investigations of source properties

The performance of the orthogonal source was tested after being mounted (see Fig. 2) onto a double-stage reflectron time-of-flight mass analyzer of 1.3 m length, which was originally built for an electrospray ion source [14]. The ion signals were formed by a channel-plate detector with good timing characteristics and a constant fraction discriminator and recorded in a time-to-digital converter in channels of 0.5 ns width. In this case an extracting field strength  $E \approx 170$  V/mm was applied over 6 mm for about 5  $\mu$ s with a repetition rate of 3.3 kHz. Fig. 4 shows the mass spectrum obtained with SF<sub>6</sub>. The mass 127 u was recorded with a peak width of less than 2 ns after a flight time of  $\approx 33$   $\mu$ s. This corresponds to a mass resolving power of  $m/\Delta m \geq 10\,000$ . This experimentally obtained line width corresponds to turn-around-times between the two values for  $\Delta t_v$  of Table 1. This indicates that the initial orthogonal ion velocity  $v_0$  is substantially reduced compared to thermal velocities. For heavier ions higher mass resolving powers were obtained since in those cases the overall flight times are longer and constant timing errors in our recording electronics play a smaller role. This indicates that other timing errors than the turn around time are dominating.

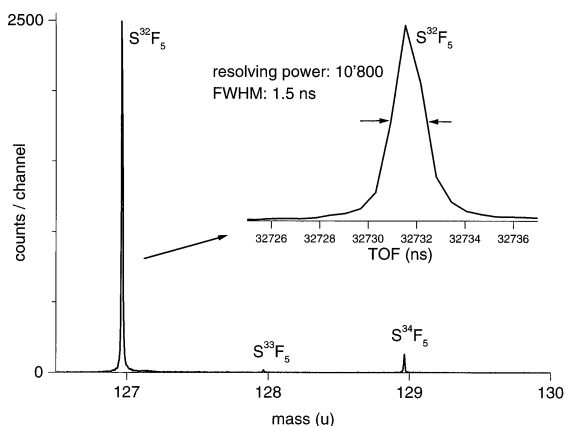


Fig. 4. Some fragments of  $\text{SF}_6$  recorded in the time focus of our reflectron time-of-flight mass analyzer (see Fig. 2) with the ion produced in the source shown in Fig. 1.

The detection limit has been evaluated with the line of  $^{16}\text{O}^{18}\text{O}^+$  (34 u). We used a 50% air and 50% helium mixture, a source pressure of  $8 \times 10^{-6}$  mbar and emission current of  $50 \mu\text{A}$ . With a natural abundance ratio of  $^{18}\text{O}/^{16}\text{O}$  of 0.2% the mass 34 molecules correspond to 400 ppm. When  $10^6$  spectra are accumulated we find 1 ppm corresponding to about 80 ions (Fig. 5) ( $10^6$  spectra can be accumulated

in 10 s when an extraction frequency of 100 kHz is applied). The best background is as low as 0.25 counts/channel which corresponds to 2.5 ppb, but this detection limit is only reached far away from abundant mass peaks: the background caused by tails from adjacent mass peaks is much higher in most parts of the spectrum. We assume that these tails arise from collisions with the grids and the low detection limit should be reached on the whole spectrum when using a gridless reflector. Pulsing of the primary ion beam (Sec. 2.3) will additionally lower the detection limit by selecting only the mass ranges of interest and thus preventing abundant masses from entering the drift region. The enlarged sections at 45 and 49 u in Fig. 5. show that with our mass resolving power of 10 000 it is possible to distinguish molecules which have the same mass number by the mass defects of their constituents. The mass accuracy is about one 1/1000 u.

#### 4. Conclusion

With integration of an electron impact gas ion source in a reflectron time-of-flight mass analyzer mass resolving powers of  $m/\Delta m \geq 10\,000$  for the

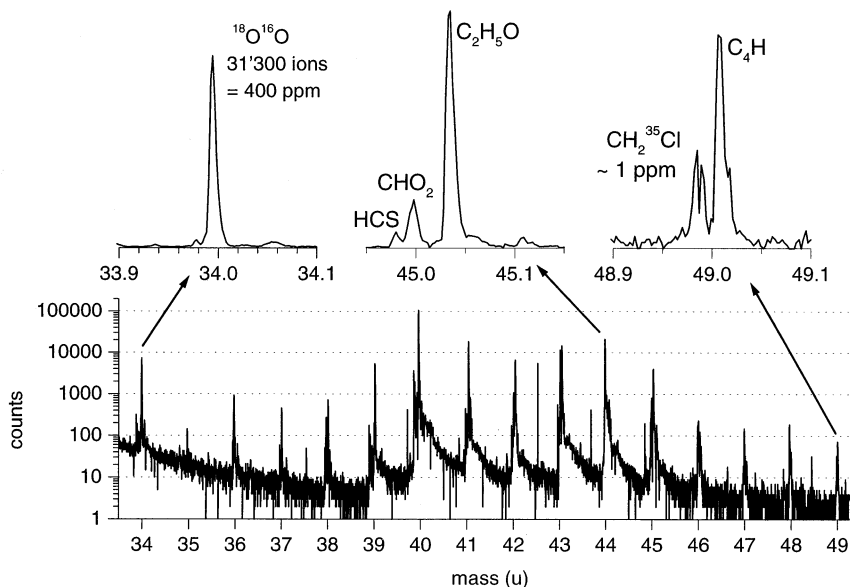


Fig. 5. The mass spectrum of a 50/50 He–air mixture in the mass range from 34 to 49 u.

mass-127 u peak could be achieved. This is to our knowledge the highest resolving power obtained so far with a TOF MS in combination with electron impact ionization. The best detection limit is in the low ppb range when  $10^6$  spectra are accumulated and might be further reduced with a pulsed primary beam and a gridless reflector.

### Acknowledgements

Support by the German Volkswagenstiftung, the Swiss National Foundation (SNF) and the Taiwan National Science Council is gratefully acknowledged.

### References

- [1] D. Price, G.J. Milnes, *Int. J. Mass Spectrom. Ion Processes* 99 (1990) 1.
- [2] W.C. Wiley, I.H. McLaren, *Rev. Sci. Instrum.* 26 (1955) 1150.
- [3] B.A. Mamyrin, D.V. Karataev, D.V. Shmikk, and V.A. Zagulin, *Sov. Phys. JETP* 37 (1973) 45.
- [4] H. Wollnik, *Mass Spec. Rev.* 12 (1993) 89.
- [5] R.B. Opsal, K.G. Owens, J.P. Reilly, *Anal. Chem.* 57 (1985) 1884.
- [6] G.J. O'Halloran, R.A. Fluegge, J.F. Betts, W.L. Everett, Rep. ASD-TDR 62-644, Bendix Co. Res. Lab., 1964.
- [7] U. Boesl, H.J. Neusser, R. Weinkauff, E.W. Schlag, *J. Phys. Chem.* 86 (1982) 4857.
- [8] A.F. Dodonov, I.V. Chernushevich, T.F. Dodonova, V.V. Raznikov, V.L. Talrose, Patent No. SU 1681340A1 (1987).
- [9] J.H.J. Dawson, M. Guilhaus, *Rapid Comm. Mass Spectr.* 3 (1989) 155.
- [10] A.F. Dodonov, I.V. Chernushevich, V.V. Laiko, in *Time-of-Flight Mass Spectrometry*, R.J. Cotter (Ed.), American Chemical Society, Washington, DC, 1994, p. 108.
- [11] J. Coles, M. Guilhaus, *Trends Anal. Chem.* 12 (1993) 203.
- [12] T. Bergmann, T.P. Martin, H. Schaber, *Rev. Sci. Instrum.* 60 (1989) 792.
- [13] D.A. Dahl, SIMION 3D Version 6.0, 43rd ASMS Conf. Proc. 1995, p. 717.
- [14] A. Dodonov, V. Kozlovski, A. Loboda, V. Raznikov, I. Sulimenkov, A. Tolmachev, A. Kraft, H. Wollnik, *Rapid Comm. Mass Spectr.* 11 (1997) 1649.